orthogonal to the direction of flow. This approach can provide higher throughput and sensitivity of detection of malaria as compared to the current frontline approaches and can also be used for diagnosis of other diseases that results in changes in the elasticity of RBC membrane, like leukemia.

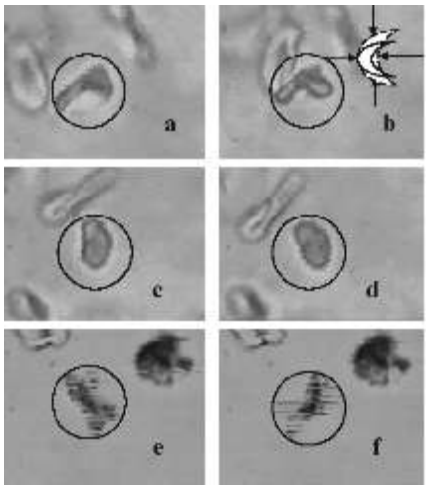

Fig. L.7.1 Rotation of a normal RBC trapped by optical tweezers. The cell (encircled) was suspended in a hypertonic buffer and trapped at power levels that varied from (a) 40 mW to (b) 200 mW. Figure 1(b) inset shows a schematic of the deformation observed in the horizontal cross section of a RBC structure at a higher trap beam power (solid curve). The dotted curve corresponds to the shape observed without the trapping beam. Arrows illustrate the transverse gradient force of optical tweezers. (c) and (d) show time-lapsed digitized video images of RBC rotation at a buffer osmolarity of 1,000 mOsm/kg; images in (e) and (f) represent an osmolarity of 1,250 mOsm/kg. The trap power was 80 mW and the time lapse between consecutive frames was 80 ms. The speed of rotation was estimated to be 25 rpm at 1,000 mOsm/kg and 200 rpm at 1,250 mOsm/kg.

(Contributed by: S.K Mohanty, A. Uppal,
P. K. Gupta: pkgupta@cat.ernet.in)

L.8 Rotation of transparent, non-birefringent objects by transfer of optical spin angular momentum

Transfer of light angular momentum to trapped objects is being actively investigated both from the point of view of fundamental understanding of the process and the potential of this transfer for realization of all optically driven micro machines. Control of rotation speed in optically driven micro machines using orbital angular momentum transfer requires a change in the power of trapping beam which may not be desirable because of possible adverse effects on the rotating object(s) at higher power levels. In this respect optically driven micro machines using transfer of light spin angular momentum have the advantage in that their rotation speed can be controlled by a control on ellipticity of the trap beam. However, so far transfer of spin angular momentum of light has been reported only for those cases where the object is birefringent or absorbing. Transfer of spin angular momentum should also occur if the incident and emerging rays are in different directions. An angular momentum equal and opposite of the vector difference between the spin angular momentum of the emergent and incident rays should act on the trapped object. For the case of a spherically symmetric objects, trapped in equilibrium position with its center coincident with geometrical focus of trapping beam there is no change in the direction of the trapping rays and hence there is no transfer of angular momentum. It is perhaps for this reason that transfer of spin angular momentum to transparent non-birefringent objects was not attempted.

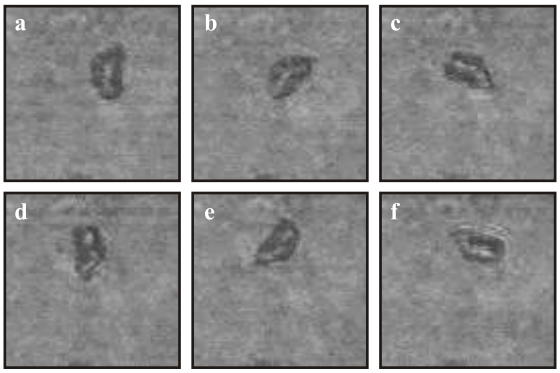

Fig L.8.1 *Digitized time laps images of rotating $NaBrO_3$ crystal*

We analyzed propagation of elliptically polarized light through isotropic objects of different shapes trapped in equilibrium configuration and found that the change in the direction of the incident and the refracted rays is particularly significant in case of a tetrahedral shaped object. Therefore, to demonstrate the effect we selected an isotropic tetrahedral crystal i.e. sodium bromate. We selected 1-octanol (η_o=1.428) as the surrounding medium because it has a lower index of refraction compared to sodium bromate, no chemical reactivity with sodium bromate and its high viscosity (η_o=10.6 cP) prevents the small sodium bromate crystals (specific gravity = 3.39) from settling down quickly on the cover glass and get attached to the surface by strong Van der Waals force. In order to observe the rotation of this crystal by transfer of spin angular momentum from the trapping beam we used a conventional laser tweezers set up. For trapping beam power of ~ 32mW at the specimen plane the experimentally observed rotational frequency was 0.21 Hz in reasonable agreement with our estimates (Fig. L.8.1). In fig. L.8.2 we show the change affected in the rotational speed of the trapped object by a change in the ellipticity of polarization

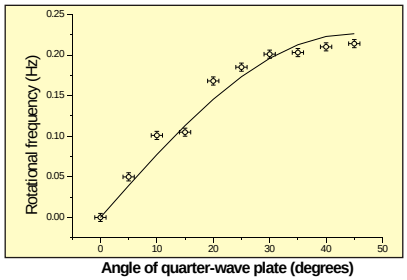

Fig. L.8.2 *Variation of rotational frequency with changing angle of the quarter-wave plate*

of the beam. The ellipticity of polarization of the trap beam was changed by placing a quarter-wave plate in the path of the trapping beam and changing the orientation of its fast axis with respect to the polarization plane of the beam. [R Dasgupta and P K Gupta, to appear in Opt. Lett.].

(Contributed by: R. Dasgupta and P. K. Gupta;
pkgupta@cat.ernet.in)

L.9 All-optical switching with metalloporphyrins

Considerable research efforts are directed towards all-optical molecular devices for information processing and storage that offer advantages of small size and weight. Metalloporphyrins are interesting chronophers due to their large nonlinearity and amenability to tailoring of their properties by different techniques to develop better materials for device applications. Vanadium (IV)-oxide tetraphenylporphyrin (VOTPP) and Zinc (II) tetraphenylporphyrin (ZnTPP) show enhanced nonlinear optical properties. All-optical switch is a fundamental building block of information processing for future.

All-optical switching experiments were performed in ZnTPP and VOTPP in toluene solution using pump probe method. A He-Ne laser of 633nm was used as probe beam and a flash lamp pumped frequency doubled Q-switched Nd:YAG laser of 532nm, 20ns pulse width was used as the pump beam. Fig. L.9.1 (a) and (b) show all optical switching characteristics of ZnTPP and VOTPP, respectively. Switch 'off' and 'on' time for ZnTPP are ~200ns and ~3.5ms respectively and for VOTPP respective times are ~1.5ms and ~2.5ms. Further, the effect of variation of pump energy on transmitted probe beam intensity for different concentrations of VOTPP was also studied. Results indicate that there is an optimum value of concentration (43% linear transmission at 532 nm) for which maximum modulation of the probe beam (~30%) was achieved with 1.1 mJ pump energy. Fig. L.9.1 shows larger fall time of VOTPP in comparison to ZnTPP. Rate equation approach was used to analyze the observed switching characteristics of ZnTPP and VOTPP. Theoretical switching curve for ZnTPP, using three states model, was in good agreement with the experimental result. However, for VOTPP the comparison of switching dynamics obtained by theoretical simulations and experimental data pointed out the possibility of existence of an intermediate state, so called charge transfer state with ~1.5ms lifetime.

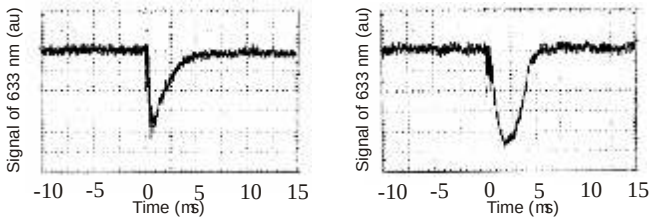

Fig. L.9.1 All-optical switching in (a) ZnTPP and (b) VOTPP.

Since the kinetic and spectral properties of metalloporphyrins can be tailored by different means, the switching characteristics can be optimized for desired applications. In an ideal case, where the probe beam does not get absorbed by the ground state, complete switching (100% modulation of the probe beam) can be achieved by increasing the input intensity. The switching operation can be made fast by decreasing the lifetime of triplet state. Metalloporphyrins based switches would be potentially useful in optical signal processing. They can provide an alternative to the thermo-optic, MEMS, and liquid crystal switches that operate in the ms range.

(Contributed by: C.P Singh, K.S. Bindra and S.M. Oak;
oak@cat.ernet.in)

L.10 Laser surface treatment enhances localized corrosion resistance of austenitic stainless steel

Austenitic stainless steels (ASS) are susceptible to localized corrosion in chloride bearing environment. Super ASS with high concentrations of Cr (» 25%) and Mo (» 6.5 %) exhibit superior corrosion resistance than the popular 18/8 variety of SS. Surface alloying of ASS with Cr and Mo, therefore, offers an economical means of enhancing corrosion resistance of relatively cheaper 18/8 stainless steel.

With this objective in mind, laser surface alloying experiments were carried out with indigenously developed 2.5kW CW CO_2 laser. The modification of surface chemical composition of type 304L SS was effected by laser deposition with pre-mixed powders of type 316L SS and Cr. For controlling ferrite content arising out of Cr alloying, laser deposition was also performed with premixed powders of type